Radiocarbon, Vol 61, Nr 3, 2019, p 799–815 DOI:10.1017/RDC.2019.29

MODELED AND MEASURED CARBON ISOTOPIC COMPOSITION AND PETROGRAPHICALLY ESTIMATED BINDER-AGGREGATE RATIO—RECIPE FOR BINDING MATERIAL DATING?

Danuta Michalska[1]* · Jacek Pawlyta[2]

[1]Institute of Geology, Faculty of Geographical and Geological Sciences, Adam Mickiewicz University, ul. Bogumiła Krygowskiego 12, 61-680 Poznań, Poland
[2]Institute of Physics - Centre for Science and Education, Silesian University of Technology, Konarskiego 22B, 44-100 Gliwice, Poland

ABSTRACT. This paper presents the results of radiocarbon (^{14}C) dating of bulk mortars and reports an attempt of implementation of the knowledge about the isotopic fractionation, based on $\delta^{13}C$ measurements, to make the age correction for mortars, together with verification of such correction based on the percentage estimation of carbonate components, namely binder and aggregate. To evaluate the variability of isotopic fractionation during CO_2 absorption by mortar, dependent on the climatic and environmental conditions, and the type of mortar, the $\delta^{13}C$ measurements have been performed for the mortars from Sussita (Golan Heights). Such measurements were also made for fragments of natural carbonate rocks and for mortars produced in the laboratory from the same substrate. We propose the recipe for mortars age estimation.

KEYWORDS: carbon isotopic fractionation in mortars, mortar age correction, petrographic observation of mortars, radiocarbon dating of mortars, $\delta^{13}C$ of mortar components.

INTRODUCTION

Carbonate binding materials used in building construction, if appropriate preparatory procedures are applied, can be an excellent substance for radiocarbon (^{14}C) dating—depending on their detailed composition. This is enabled by absorption of CO_2 from the air during their hardening process, and thereby by binding of the isotope ^{14}C. Mortars are a mixture of binder and aggregate in various proportions. Their age is strictly connected with the time of building construction. The difficulty in dating of carbonate mortars and plasters comes from possible content of carbonates of different origin, which were not involved in the burning process (e.g. aggregate, partially burnt fragments, powdered admixtures reacting with carbonates) and, as a consequence, they did not absorb CO_2 during hardening. The presence of carbonate aggregate in the binder may have a significant impact on the result of the ^{14}C dating, causing the effect of ageing of the dated sample (Baxter and Walton 1970; Van Strydonck et al. 1986; Heinemeier et al. 1997, 2010; Nawrocka et al. 2005, 2009; Lindroos et al. 2007, 2011, 2014; Michalska Nawrocka et al. 2007; Goslar et al. 2009; Ringbom et al. 2011, 2014; Hajdas et al. 2012, 2017; Michalska et al. 2013; Nonni et al. 2013). Hence, comes the necessity of eliminating it in the stage of preparation of the sample for measuring (Nawrocka et al. 2009; Marzaioli et al. 2011, 2013; Ringbom et al. 2011; Michalska and Czernik 2015; Hajdas et al. 2017). Mortars may contain aggregate of various fractions, composition and proportions in relation to the binder. In the case of very fine aggregate, the elimination of the carbonate contamination is extremely difficult, depending on the type and the state of preservation of the research material.

Additional factors influencing ^{14}C age are not fully burnt fragments of carbonate rocks, which occur in a dated mortar. Secondary crystallization of carbonates (not observed in the dated samples), can also modify the ^{14}C age, depending on geoenvironmental conditions, or as a result of reaction between mortar carbonates and additives, e.g. crushed bricks, ceramics, etc.

Charcoal from mortars, often used as a comparative material, should also follow proper preparation procedure, depending on its level of preservation and environmental conditions

*Corresponding author. Email: danamich@amu.edu.pl.

of its location (Berger 1992; Cohen-Ofri et al. 2006; Rebollo et al. 2008). Complications with charcoal dating are connected not only with the risk of its origin from old wood, and in consequence with the date over-aging referring to a real time of construction of a building, from which the mortar was sampled. Depending on the conditions experienced by a sample, charcoal may also reflect an effect typical for activated carbon. Such presumption would explain the diversity of ^{14}C dates obtained from charcoal pieces extracted from the same mortar, when their ages differ not only from the binder age, but also from each other (Hajdas et al. 2017; Michalska et al. 2017).

An inseparable relation between mortars and the time of construction of a building makes it important to find the methodology, which allows for obtaining the true age of their production (Michalska et al. 2013). It is an extremely difficult task, due to the composition of mortars, which is differentiated and most often connected with local geological structure, meaning the access to raw materials used for making mortars. Recent studies are focused mainly on establishing preparatory procedures appropriate for a given type of mortar, starting with dating of specific grain fractions, followed by sequential dissolution of grain fractions, up to dating of different portions of suspension from a mortar (Michalska et al. 2017). Another interesting issue is the isotopic fractionation connected with the process of mortar production (Pachiaudi et al. 1986; Ambers 1987; Van Strydonck et al. 1989; Michalska and Czernik 2015).

This paper presents the results of ^{14}C dating of bulk mortars and reports an attempt of implementation of the knowledge about the isotope fractionation, based on $\delta^{13}C$ measurements, to make the "reservoir" age correction for mortars. Verification of such correction has been based on the percentage estimation of specific carbonate components in mortars using petrographic studies. The $\delta^{13}C$ measurements and ^{14}C dating have been performed both for the mortars and plasters from Sussita, as well as for experimental mortars. This work is of a methodological aspect and refers to the possibility of age modeling on the basis of $\delta^{13}C$ measurement and the sample composition.

HISTORICAL DEVELOPMENT OF THE SETTLEMENT

On the eastern shore of the Sea of Galilee (Lake Kinneret), on a hill, about 350 m above the lake surface, an ancient city Sussita (in Aramaic, in Greek named "Hippos") is located. It lies about 2 km east from the modern city of En Gev (Figure 1). One of the oldest historical sources mentioning Sussita is *Historia naturalis* by Pliny the Elder, which indicates the city affiliation with Decapolis. The excavations conducted there allowed for determining the history of the city. It was founded in 3rd cent. BC, during the reign of Rome it belonged to the group of cities Decapolis, and in the Byzantine times (5th–6th AD) Sussita prospered as a bishopric capital. In the 7th century, the Sasanian invasions of Levant, and later Islamic conquest could lead to desolation of the city. Finally, Sussita was destroyed by an earthquake in 749 AD.

Most of the samples were taken from North-Western Church and its immediate surroundings. The North-Western Church is a three-nave basilica preceded by a square, cobbled courtyard. One sample comes from the church on the eastern side of the settlement (North-Eastern Church). Previous archaeological survey allowed to distinguish three chronological phases of the North-Western church. Phase I was connected with building of the church (around 5th century AD); phase II: dated to the end of the 6th century due to a wide range of decorative motifs occurring in mosaic floors and phase III included expanding the presbytery through installing balustrades in the aisles, most probably in the 7th century. The church functioned

https://doi.org/10.1017/RDC.2019.29 Published online by Cambridge University Press

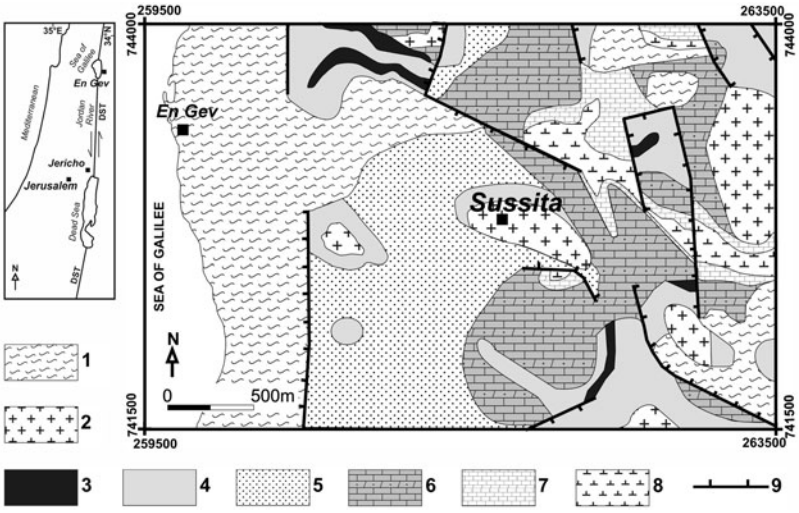

Figure 1 General view of research area together with simplified geological map of Sussita region (modified after Geological Survey of Israel 2008; Mor et al. 1997; Shtober-Zisu 2013); DST—Dead Sea Transform (Eppelbaum et al. 2004); 1–Alluvium; 2–Cover Basalt, Pliocene; 3–Lower Basalt Fm., Middle-Late Miocene; 4–Hordos Fm., Middle-Late Miocene, conglomerates, calcareous sandstones, marly chalks, marls; 5–En Gev Fm., Middle Miocene, sandstones and sandy limestones, limestones and marls; 6–Sussita Fm., Oligocene-Early Miocene, limestones, marls, sandy dolomites, cherts; 7–Fiq Fm, Late Eocene-Oligocene, limestones rich in marine microfauna, chalks, marls; 8–Maresha Fm., Middle Eocene, chalk; 9–fault.

until the earthquake in 749. The south wall of North-Western church touches such devices as olive press and wine press, contemporary to II or even III phase of the basilica. This church was raised on an earlier, Roman temple (Młynarczyk 2000; Segal et al. 2004).

GEOLOGY OF THE AREA

In the aspect of the petrographic studies, as well as the isotopic fractionation measurements, a significant part of research is examination of the local geology. This knowledge gives an insight to the information about the raw materials used for mortars production. Sussita is located on the eastern shore of the Sea of Galilee, on the western slopes of the Golan Heights, almost entirely encircled by mountains. The Sea of Galilee is located in the northern part of the Jordan Rift Valley. This ancient site is located on the flat-topped mountain, at an altitude of 142 m asl (Shtober-Zisu 2013).

The Golan Heights are the volcanic plateau with the lava flows covering older geological structures (Mor et al. 1997). Two main phases of basaltic volcanism can be distinguished in the area of the Sea of Galilee: Early-Cretaceous and Late-Cenozoic (from Miocene to Pleistocene). The first one gives in the lake area the lowest thickness in the Northern Israel. The majority of basaltic exposures is therefore of the Pliocene-Pleistocene age. In the discussed area, several fault systems/zones have been distinguished (Eppelbaum et al. 2004; Meiler 2011). The Sea of Galilee is a part of a N–S extended pull-apart basin. There are a few such tectonic structures along the Dead Sea Transform fault system (Garfunkel, 1981; Ben-Avraham et al. 2005; Katz et al. 2011). Several large historic earthquakes in this

https://doi.org/10.1017/RDC.2019.29 Published online by Cambridge University Press

region are the results of tectonic activity of the Jordan Valley Fault (Ben-Menahem 1991; Guidoboni et al. 1994; Guidoboni and Comastri 2005). The most destructive earthquake in the discussed area occurred in 749 AD (Reches and Hoexter 1981) and caused devastation of the cities of this region, e.g. Sussita, Tiberias and the village of Umm El Qantir (Marco et al. 2003; Wechsler et al. 2009). All these settlements are located at a radial distance of less than 15 km from the Jordan Valley Fault (Katz et al. 2011).

The steep slopes of the Golan Heights falling to the shore of the Sea of Galilee are formed mainly from lacustrine and fluvial sediments of Miocene age. The area is tectonically rebuilt by numerous faults. The presented map (Figure 1) shows the geological setting of the Sussita region. The limestone formations, which could be the alimentation sources of raw material used for building construction are the Fiq Formation (Upper Eocene to Oligocene age; structure no. 7 in the Figure 1) and the concordantly overlying Sussita Formation (Oligocene do Lowest Middle Miocene; no. 6), as well as the En Gev Fm. (Middle Miocene; no. 5) or the Hordos Fm (Middle-Late Miocene; no. 4).

The Fiq Formation, which is the oldest exposed formation in this area (thickness 45 m), reaches its highest thickness in the Nahal En Gev area (Shtober-Zisu 2013). It is formed by limestones rich in marine microfauna, chalk, and marl. Glauconite rocks also occur there (glauconitic calcarenite). The Sussita Formation is built of limestones, marls, sandy dolomites, cherts, and loose yellow sands. This formation reaches its maximum thickness near Sussita (145 m). The Sussita Fm. is discordantly overlain by the En Gev Sands and Hordos Formation. The sands of En Gev represent the beginning of the continental cycle. They come from Middle-Upper Miocene. Their thickness is around 90 m and they occur in the vicinity of Sussita-Qeren, En Gev (Mor et al. 1997). The En Gev Formation is built mainly of sandstones and sandy limestones, limestones and marls (Michelson et al. 1987). The Hordos formation is composed of conglomerates, calcareous sandstones, marly chalks and marls (thickness 242 m; Meiler 2011).

The outcrops of Hordos Formation are exposed all over the surrounding of the Sea of Galilee (Shtober-Zisu 2013). These Miocene-age formations were deposited on the Eocene substratum and overlain by the Gesher Formation or capped by the Plio-Pleistocene basalt cover (Michelson et al. 1987). The Gesher Formation in the Sussita area comprises a sequence of limestones, chalks, detritic limestones and abundant clays at the top (Shaliv 1991; Shtober-Zisu 2013). The two streams, Ein Gev and Sussita, crosscut the lithological succession of the Lower and Middle Pleistocene. From one side, the Ein Gev channel gives the outcrops of the limestones belonging to the Sussita Fm., while on the second side the conglomerates are accessible at the river terraces within the Sussita channel (Shtober-Zisu 2013).

METHODS AND SAMPLES

This study aims to determine accurate ages of mortars, based on ^{14}C measurements of bulk samples, being mixtures of binder and aggregate. The obtained dates have been refined using the corrections on isotopic fractionation and mineral composition of the sample.

The petrographic observations were made using polarized light microscope Olympus AX 70-Prons and the binder-aggregate ratio were estimated with the software AnalySIS (Soft Imaging System). Mortars components and proportions of aggregate to binder, were additionally investigated using the scanning electron microscope with EDS microanalyzer (Hitachi S-3700N in Institute of Geology, Poznań).

https://doi.org/10.1017/RDC.2019.29 Published online by Cambridge University Press

The ^{14}C measurements have been made in the Gliwice Radiocarbon Laboratory by conventional techniques (Pazdur et al. 2000). The mortars were crushing and gridding and then total dissolution with HCl (37%) take place. Apart from ^{14}C, also $\delta^{13}C$ and $\delta^{18}O$ of bulk material were measured using standard off-line IRMS procedure and 106% H_3PO_4.

For the samples, where the separation of carbonate mortar fragments was successful, additional measurements of $\delta^{13}C$ and $\delta^{18}O$ in these fragments have been carried out (Tables 1 and 2). Stable isotope measurements were conducted in the Department of Radioisotopes, Gliwice, Institute of Physics, Silesian University of Technology, by the mass spectrometer IsoPrime coupled with MultiFlow carbonate analysis system. 103% phosphoric acid was used for carbonates decomposition. Multi-point calibration method was applied for the isotopic δ calculations.

The following samples were subjected to the latter analyses: 61H—facade of the pastophorium northern wall, 76H—floor of the first step of the wine press tank, N of of the pastophorium, 151, 2H—layer of plaster (second out of four) in the tank of the wine press, to the north of the pastophorium, A1/H—NE church, plaster from the apse, 14H—floor pour of channel exposed at the chancel area, 80H—interior of one of the twin tombs, in the "mortuary room," 5H—cistern in the church atrium, material from its inner wall (see Supplement 1). All samples were collected carefully, as close to the facade as possible, due to the possibility of delayed hardening for samples taken too deeply.

The first samples of lime mortars from Sussita, in the form of different grain fractions, have been dated using the GPC and AMS techniques in Gliwice (Gd-) and Poznań (Poz-) laboratories (Michalska Nawrocka et al. 2007). The bulk material measurements have been also supplemented by suspension dating and compared with previous charcoals and grain fraction measurements (Michalska Nawrocka et al. 2007, Figure 4). In case of the sample 61H, the thin layer of the binder that covered small pieces of basaltic aggregate (Poz-16078; Michalska Nawrocka et al. 2007) was dated. Apart from bulk mortars measurements, the suspension portions of mortar 61H was additionally dated in recent studies (Michalska 2019). The second portion of suspension—repeated suspension from mortar 61H were dated after collecting gas in a first 5 sec of leaching (Poz-97862). Whereas, for sample A1/H, the binder fraction 45–100 μm (Gd-17381) and for mortar 14H, the charcoal fragment (Poz-5088), was dated in previous studies (Michalska Nawrocka et al. 2007). The obtained calibrated age was calibrated by using OxCal 4.3 program (Bronk Ramsey 2009) and IntCal13 curve (Reimer et al. 2013).

EXPERIMENTAL AND SUSSITA BINDER

Apart from the mortars, also the rock fragments cropping out adjacent to the archaeological site, namely sandy-dolomite and dolomite (Sussita Fm.) were subjected to analyses (Table 1). To understand the mechanism of isotopic fractionation during mortars production in the Sea of Galilee area, the attempt to experimentally produce the binder made of the carbonate rocks from the outcrops near the Sussita excavation site (Sussita Fm.) has been carried out. Both the raw material (rocks) and the binder obtained from it were carefully characterized and destined for the $\delta^{13}C$ and $\delta^{18}O$ measurements. The binders were made without aggregate admixture, to eliminate the measurement disturbances, to preserve the homogeneity of a sample, and to avoid influence of fossil carbon.

A thin layer of binder (estimated at 0.5–2 mm) has been produced, in order to guarantee the fast binding process, which would take part uniformly in the entire sample. The studied samples

https://doi.org/10.1017/RDC.2019.29 Published online by Cambridge University Press

Table 1 The isotopic composition measurements for different samples (for average values for binder from chosen mortars, see Supplement 1); SD—Standard Deviation. Both experimental binders were produced (from Sussita raw material) in Polish climate conditions. As comparison, the $\delta^{13}C$ of binder for sample 10H (pure finishing plaster devoid of aggregate, containing only carbonaceous binder and the empty spaces after straw), is 9.93‰VPDB (from –9.5 to –10.35‰VPDB, Michalska Nawrocka et al. 2007).

Description	Name	Lab no.	$\delta^{13}C$ (‰ VPDB)	SD ($\delta^{13}C$) (‰)	$\delta^{18}O$ (‰ VPDB)	SD ($\delta^{18}O$) (‰)	Number of subsamples
Chosen material from geological outcrops in Sussita region and experimental binder							
Dolomite	DGOL1	GdMS-54140	–7.81	0.03	–2.03	0.10	3
Experimental binder from burning of dolomite	B_DGOL1_k	GdMS-54143	–22.1	1.4	–15.19	0.21	2
Sandy dolomite	SGOL2	GdMS-54176	–8.43	0.10	–3.92	0.10	1
Experimental binder from burning of sandy dolomite	B_SGOL2_k	GdMS-54177	–25.6	1.1	–17.10	0.12	3
Sussita historic mortars							
80–100 μm dry-sieved grain fraction from mortar 61H	61H_80–100	GdMS-54150	–10.61	0.14	–13.75	0.12	2
Suspension from mortar 61H collected after 10 minutes of sedimentation	61H_sus1	GdMS-54146	–8.48	0.12	–11.52	0.12	3
Second portion of suspension from mortar 61H (repeated suspension); after pouring off susp1	61H_sus2	GdMS-54149	–8.87	0.10	–11.84	0.10	1
Plaster A1, fraction >100 μm	A1/H_>100	GdMS-54153	–14.35	0.10	–17.07	0.10	1
Binder of A1 separated under binocular	A1/b	GdMS-54583	–15.35	0.10	–17.64	0.10	1
Second portion of suspension from mortar 14H	14H/sus2	GdMS-54587	–19.51	0.10	–9.84	0.20	1
Binder of 14H separated under binocular	14H/sp	GdMS-54589	–15.31	0.10	–8.68	0.20	2
Binder of Hip80 separated under binocular	80H_B	GdMS-54156	–21.68	0.10	–14.30	0.10	1

Table 2 ^{14}C measurements results together with corrected ages of mortars. The age correction for bulk material was possible using the calculations presented in Eq. (1.1–1.5). Uncertainty for both $\delta^{13}C$ and $\delta^{18}O$ determinations of bulk material was equal or better than 0.1‰. Measured $\delta^{13}C$ of different samples are placed in Table 1, and the average measured $\delta^{13}C$ of binder for each mortar are presented in Supplement 1; IRMS—stable isotope ratio mass spectrometry.

						Based on petrography					Based on modeled carbon isotopic composition				Based on measured carbon isotopic composition of binder (IRMS)		
Lab no.	Sample name	$\delta^{13}C$ (‰) VPDB	$\delta^{18}O$ (‰) VPDB	^{14}C concentration (pMC)	Age ^{14}C (BP)	Carbon mass in aggregate to the total mass of carbon in bulk material (%)	Carbon mass percentage in the binder (%)	Estimated ^{14}C concentration in binder (pMC)	^{14}C age of binder based on petrographic analyses correction (BP)	Modeled $\delta^{13}C$ of binder (‰)	Carbon mass percentage in the binder (%)	Modeled (corrected) ^{14}C concentration (pMC)	^{14}C age of binder (BP)	$\delta^{13}C$ of binder from measurements (‰ VPDB)	Carbon mass percentage in the binder (%)	Corrected ^{14}C concentration in binder (pMC)	^{14}C age of binder (BP)
Gd-12824	61H /tot	–7.41	–9.04	41.1 ± 0.45	7140 ± 90	50	50	82.20	1575	–9.40	50	82.45	1500	–9.32	51	81.36	1657
Gd-12825	76H /tot	–13.55	–9.13	68.27 ± 0.38	3070 ± 45	20	80	85.34	1274	–15.54	80	85.05	1300	—	—	—	—
Gd-12826	151,2H/tot	–11.64	–7.8	53.69 ± 0.45	5000 ± 70	36	64	83.89	1411	–15.13	64	84.01	1400	—	—	—	—
Gd-12829	A1/ H/tot	–13.76	–16.75	71.64 ± 0.49	2680 ± 55	15	85	84.28	1374	–15.32	84	85.06	1300	–15.35	84	85.40	1268
Gd-15887	14H /tot	–12.94	–8.21	51.8 ± 0.51	5280 ± 80	34	66	78.48	1946	–16.79	66	77.45	1950	–17.41	63	82.76	1520
Gd-15888	80H /tot	–14.52	–7.77	49.32 ± 0.6	5680 ± 100	40	60	82.20	1575	–20.61	60	82.45	1550	–21.68	56	88.30	1000
Gd-12828	5H /tot	–13.49	–11.19	36.1 ± 0.46	8180 ± 100	56	44	82.05	1590	–23.80	44	82.45	1550	—	—	—	—
Aggregate	61H/A	–5.46	–5.6														

have been kept in aerial conditions, at room temperature, i.e. close to the expected temperatures of mortars stiffening and carbonation, during the historical times in Israel. The selected carbonate rocks from the Sussita area have been burnt for ten hours in 950ºC. In this process, quicklime (CaO) is formed, which after the contact with water transforms into $Ca(OH)_2$. The latter is an exothermic reaction. As in case of historical mortars, during the production of their experimental analogues, the water was added in excess, to achieve the complete reaction and to make the slurry more feasible. All efforts have been made to obtain the highest possible homogeneity of the experimental samples, apart from the diversity connected to the composition of raw material, that means of the carbonate rocks.

We tried to exclude some aspects mentioned by Van Strydonck et al. (1989), e.g. reaction kinetics controlled by the exhaustion of the reagents as a function of depth, the diffusion rate as a function of the partial pressure of CO_2 in the atmosphere, the permeability of the mortar and the amount of $Ca(OH)_2$ in a sample. We made a very thin layer of binder, which has been left in the open space without unidirectional wind, sheltered from rainfalls, until it bound and hardened. In the present research, we do not try to compare the samples' state of calcination dependent on depth, or composition, but rather to apply the isotopic fractionation measurements for the correction of ^{14}C ages. To make the wide comparison, not only the natural samples of carbonate rocks, and the experimental binders produced from them, but also the archaeological samples (61H, A1/H, 151,2H, 14H, 80H, Table 1) have been subjected to the isotopic measurements.

PETROGRAPHY (CHARACTERISTIC) OF SAMPLES

The presented outline of the geology of the area and the description of the formations occurring in the vicinity of Sussita shows the available raw materials. The reflection of the local geological structure can be clearly found in the aggregate (Figure 2). Taking into account the geological setting of the study area, and petrography of both the historical mortars and the rocks used for their production, the mortars could contain, apart from lime and dolomitic binder, also basalt fragments, clay minerals and different kinds of carbonate aggregate, e.g. organogenic limestone, sandy-limestone, sandy-dolomite, marls. The estimations of the binder/carbonaceous aggregate ratio (Table 2) were based on studies of at least 2 thin sections from the same (dated) mortar. The uncertainties of estimation of binder/aggerate ratio for dated mortar were ca. 1%.

MODELING OF $\delta^{13}C$ IN BINDERS AND AGE CORRECTION

Petrographic observations indicate different proportions, size, and type of the aggregate used in mortars and plasters, hence a significant discrepancy of the obtained results for bulk mortars with historical age is observed. The shift in ages varies for different mortars from ca. 1000 (A1/H) up to 6000 (5H) years toward older ages. Moreover, it is expected to see discrepancies between dating results for mortars with different proportion of binder to aggregate (Table 2, Figure 3). As the samples were dated in the bulk form (lime binder with carbonate aggregate), it was necessary to implement the correction for the content of carbonates from the different source that the binder.

An attempt has been made to correct the ages obtained for the samples of mortars dated in bulk form, using the data related to the carbon isotopic composition, which is reflected by the $\delta^{13}C$.

https://doi.org/10.1017/RDC.2019.29 Published online by Cambridge University Press

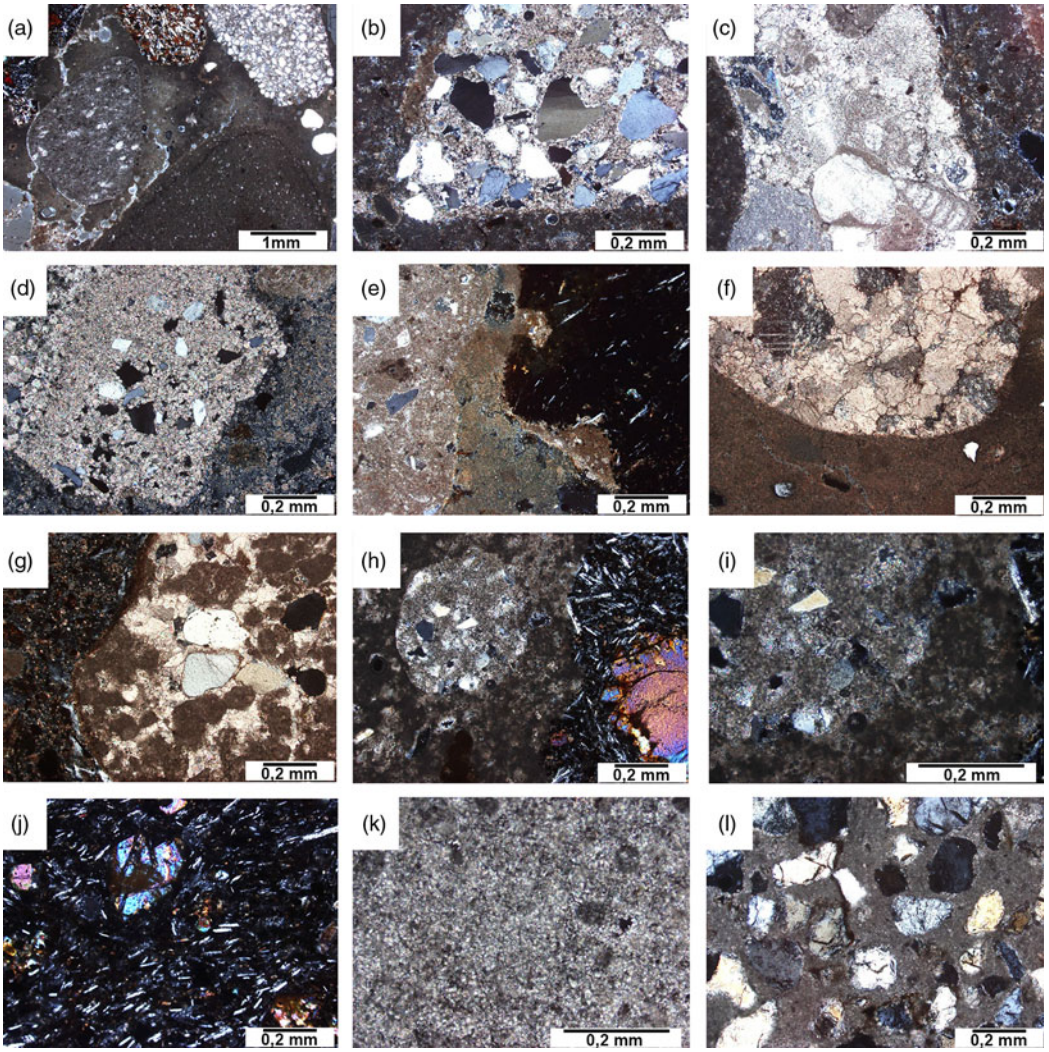

Figure 2 Petrography of analyzed mortars and raw material. A–61H with basalt fragments and different carbonaceous aggregate (sandy dolomite, limestone, marly limestone); B, C–carbonaceous aggregate from mortar 76H; B–sandy dolomite as aggregate; C–organogenic limestone; D–151,2H, the layered carbonaceous rock; E–mortar 5H, sandy dolomite and volcanic rock aggregate; F–A1/H with carbonaceous aggregate (marble?); G–14H, with aggregate of carbonaceous rock with singular quartz (siderite); H, I–80H with sandy dolomite aggregate and basalt fragments (H); J–basalt from Sussita hill with visible olivine and iddingsite; K–DGol-dolomite from Sussita Fm; L–SGol-sandy dolomite from Sussita Fm (used for experimental research).

$\delta^{13}C$ of the aggregate extracted from the 61H\K and for all the bulk sample have been measured by the isotope ratio mass spectrometer, whereas the indispensable value of $\delta^{13}C$ for the binder has been modeled using Microsoft Excel's solver module. The $\delta^{13}C$ of binder has been modeled so that the corrected ^{14}C age of mortar matched the archaeological context. $\delta^{13}C$ of the 61H\K aggregate (–5.46‰VPDB) was used when modeling $\delta^{13}C$ of the binders. This attempt allows to observe that the ratio of carbonaceous aggregate to binder estimated on the basis on modeled $\delta^{13}C$ are similar to those obtained independently from petrographical research. The amounts of binders and aggregate in mortars acquired using

https://doi.org/10.1017/RDC.2019.29 Published online by Cambridge University Press

the $\delta^{13}C$ values, were verified by the estimated percentage of these components (Table 2) resulting from petrographic observations, made with the software AnalySIS (Soft Imaging System).

For the samples where enough material was available, the binder modeled $\delta^{13}C$ (Table 2, column 11) was compared to $\delta^{13}C$ from measurement (IRMS, Table 2, column 15).

Considering all the necessary procedures required for the ^{14}C age calculation (Stuiver and Polach, 1977), the age correction for binder and aggregate was possible using the following calculations:

$$\frac{\delta^{13}C_b - \delta^{13}C_a}{\delta^{13}C_{bi} - \delta^{13}C_a} = \frac{m_{bi}}{m_b} \tag{1.1}$$

$$\delta^{13}C_b = \frac{\delta^{13}C_a \times m_a}{m_b} + \frac{\delta^{13}C_{bi} \times m_{bi}}{m_b} \tag{1.2}$$

$$A_{bi} = A_b \frac{m_b}{m_{bi}} \tag{1.3}$$

$$A_{bi} = A_b \frac{\delta^{13}C_{bi} - \delta^{13}C_a}{\delta^{13}C_b - \delta^{13}C_a} \tag{1.4}$$

$$t_{bi} = -8033 \times \ln \frac{A_C \frac{m_b}{m_{bi}}}{A_{std}} \tag{1.5}$$

where:

A—specific ^{14}C radioactivity; m—mass; a—aggregate; std—standard, bi—binder, b—bulk.

DISCUSSION OF RESULTS

The correction of conventional ages obtained from measurements made on bulk samples, depends on carbonaceous binder to aggregate ratio, environmental conditions and on local geological formations used as a raw material for mortars and plasters production. The aggregate in the Sussita samples has mainly Miocene age and from the ^{14}C dating point of view the age may be treated as infinite.

The modeled $\delta^{13}C$ values for the binder enabled estimation of the carbonate fraction percentages, which were very close to the results obtained using petrographic observations for those components. Moreover, in the all cases where IRMS measurement of binder $\delta^{13}C$ was possible, all the results (of binder to aggregate ratio) were consistent or similar with those obtained during modeling (Table 2, Supplement 1). The results of modeling (and measurements) made for different types of mortars (and plasters) show similar $\delta^{13}C$ values for each type of carbon bonding mechanism in the sample (Tables 1 and 2 and Supplement 1), e.g. for finishing plaster (Hip10, caption of Table 1) and an open-air mortar (61H) from ca. –8 to –10‰VPDB (Table 1); for mortars covered by another layer of plaster or by mosaic, ca. –15‰VPDB, and for the samples from humid and colder conditions, closer to more negative values: –20, –23‰VPDB (as for Belgium mortars; Van Strydonck et al. 1986). That kind of estimation and modeling needs verifications for mortars from different climatic conditions, however it is very promising, especially when taking into account how

https://doi.org/10.1017/RDC.2019.29 Published online by Cambridge University Press

difficult is to obtain pure binder fraction from archaeological mortar not only for ^{14}C, but also for $\delta^{13}C$ measurements. Looking on the Table 2, and Supplement 1, the $\delta^{13}C$ gives the information about the mortar type.

The conducted research proved that the isotopic fractionation distinctly differs for mortars from various climatic conditions. Referring to the measurements made by Van Strydonck et al. (1986, 1989), the fractionation in the mortars from Israel, with a high average temperature, is different than in case of the mortars produced in colder environment. Therefore, the isotopic fractionation and $\delta^{13}C$ values published by Van Strydonck et al. (1989) differ from those obtained for the historical mortars from Sussita. Such assumptions were also confirmed by the independent $\delta^{13}C$ measurements of the experimental binders produced in Polish climate conditions from the raw materials coming from the vicinity of Sussita, Israel (Table 1). The $\delta^{13}C$ values for these experimental binders are much more negative (B_DGOL1_k: –22.1‰VPDB; B_SGOL2_k: –25.6‰VPDB) than for the original historical binders formed on the site of Sussita (but similar to Van Strydonck et al. (1989) measurements of Belgium samples).

The results of ^{14}C measurements after application of the appropriate petrographic corrections enabled to establish the age, which fell into the time range of the settlement existence (Figure 3). The further discussion focused mainly on the samples for which the age correction based on measured (IRMS, Supplement 1) carbon isotopic composition, was possible (enough material was available from: 61H, A1/H, 14H, 80H). For all samples, the corrected ^{14}C age and the binder-aggregate ratio based on two different assumptions ("petro" and "model"), could be observed in Table 2.

For the mortar 61H, the obtained corrected age of this sample which was measured as bulk material, together with measurements of different portion of suspension from the same mortars revised the previous hypothesis regarding the age of this mortar (Michalska Nawrocka et al. 2007). The real age of mortar 61H obtained by ^{14}C measurement of the second portion of suspension with CO_2 collected in the first 5 sec of leaching reaction (61H/sus2/0-5s, Poz-97862, 1470 ± 30 BP; Michalska 2019), together with measurements of thin layer of binder covering basaltic aggregate (61H/>100, Poz-16078, 1490 ± 30 BP; Michalska Nawrocka et al. 2007) were verified (Figure 4) by the results obtained by application of appropriate corrections (61H/tot/petro: 1575 ± 90BP, 61H/tot/IRMS: 1657±90 and 61H/tot/model: 1550 ± 90BP) to the bulk mortar measurement (61H/tot, Gd-12824).

Considering plaster A1 from the North-Eastern church, with the composition similar to mortars (Figure 2), the obtained corrected ages (A1/H/tot/petro: 1374±55 BP, A1/H/tot/IRMS: 1268 ± 55 BP and A1/H/tot/model: 1300 ± 55 BP, Figures 3, 4) are within the time interval specified by the relative chronology and are also similar to the previous measurements for this sample (A1/H/45-100/Gd-17381, 1140 ± 130; Michalska Nawrocka et al. 2007)

Comparing obtained corrected ages of mortar 14H (14H/tot/petro: 1946 ± 80 and 14H/tot/model: 1950 ± 80 BP) with previous charcoal dating from the same mortar (14H/ch, Poz-5088, 2025 ± 80 BP; Michalska Nawrocka et al. 2007) the convergence is also visible. The age corrected basing on measured carbon isotopic composition (14H/tot/IRMS: 1520 ± 80 BP) is shifted towards younger ages. Considering the hydraulic character and composition of that sample, the assumption, that collecting of pure binder for IRMS measurements was not possible in this case could be made. The provenance of sample 80H from humid

https://doi.org/10.1017/RDC.2019.29 Published online by Cambridge University Press

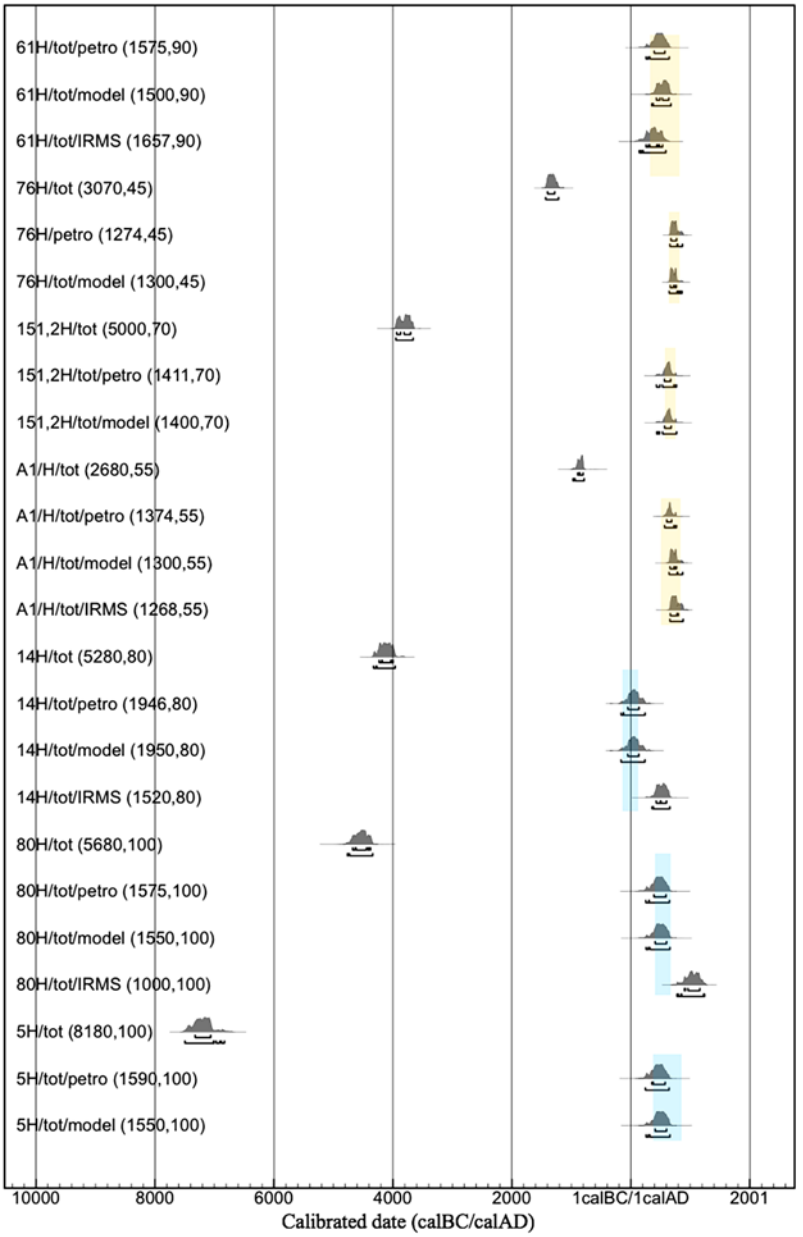

Figure 3 Calibration of the results in graphical form of bulk material and after applying the age corrections; 61H–mortar name; tot–bulk material; petro–age correction based on petrographic observation; IRMS–corrections based on measured carbon isotope composition of binder; model–corrections based on modeled $\delta^{13}C$ of binder; 61H/tot–bulk material of mortar 61H. The archeological estimations for dated samples are given in Supplement 1 and marked on the figure with shaded bars; orange bar–for air-hardening, open-air samples; blue bars–samples from humid conditions with limited airflow.

https://doi.org/10.1017/RDC.2019.29 Published online by Cambridge University Press

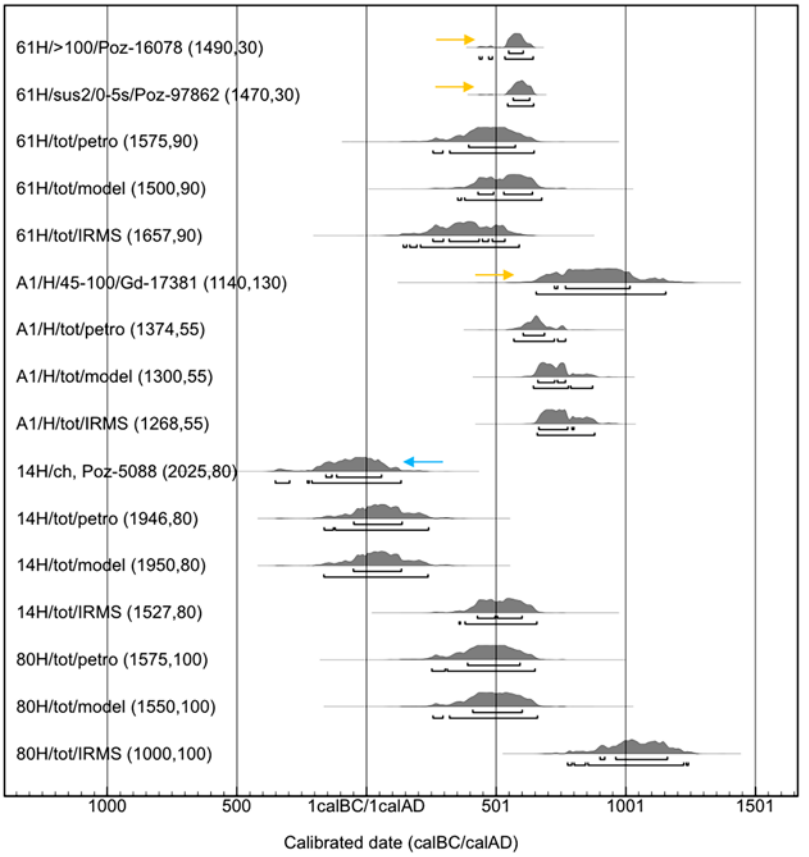

Figure 4 Calibration of ^{14}C results for mortars for which beside modeled, also measured δ13C was applied to obtain corrected ages. To verify the obtained corrected and modeled ages, the reference data are presented and marked with arrows: Poz-16078, Gd-17381, Poz-5088, Michalska Nawrocka et al. 2007, and Poz-97862, Michalska 2019); tot–bulk material; petro–age correction based on petrographic observation; IRMS–corrections based on measured carbon isotope composition of binder; model–corrections based on modeled $\delta^{13}C$ of binder; >100–separated basaltic aggregate (>100 μm) covered with film of binder; sus2/0–5s sec portion of suspension, gas collected after first 5 sec of leaching reaction; 45–100–grain fraction 45–100 μm; ch–charcoal. To distinguish the comparative, reference dates, they were additionally described by laboratory numbers and marked with arrows (a color consistent with shaded bars on Figure 3).

condition, interior of the tomb in small, closed room suggests a similar interpretation. The age obtained after correction based on measured carbon isotopic composition is also (as in 14H mortar) shifted toward younger ages (80H/tot/IRMS: 1000 ± 80 BP). The binder aggregate ratio obtained during correction based on petrography (Table 2, columns 7–8) is the same as the one obtained during modeling the $\delta^{13}C$ of binder (Table 2, column 12). However, the carbon mass percentage in the binder obtained during age correction based on measured carbon isotope composition (Table 2, column 16) is about 3–4% lower than the same parameter obtained in petrographic correction for both, 14H and 80H samples.

https://doi.org/10.1017/RDC.2019.29 Published online by Cambridge University Press

SUMMARY AND CONCLUSION

The most probable source of the raw material used for production of the studied mortars are the rocks of the Hordos Formation, cropping out all over the surrounding of the Sea of Galilee. However, some content of carbonate rocks belonging to the underlying formations (Sussita Fm. and En Gey Fm.), and cropping out at the slopes of the hill, where the historical Sussita was situated cannot also be excluded.

For samples originated from Israel or Near East in general, isotopic fractionation occurring in CO_2 fixation in binder hardening may be different than for samples in Europe. Our data may suggest that environmental conditions (not only the sample composition and type) during binder hardening in buildings construction or decoration influence carbon isotopic fractionation. The hypothesis is supported by both modeled and measured $\delta^{13}C$ of binder. Some more systematic research in laboratory controlled environments is needed to check our hypothesis.

Knowing the $\delta^{13}C$ of binder and aggregate and having a ^{14}C measurement for the bulk material, it is possible to model the actual age of the mortar. The $\delta^{13}C$ for samples of an experimental binder produced in the Polish climate from the fired rocks from the Sussita region give values similar to those defined by Van Strydonck et al. (1989). However, $\delta^{13}C$ for historic binders formed in Israel varies, depending on the mortar. In majority of cases, the $\delta^{13}C$ for binders from air-hardening mortars is close to –15.3 ± 0.2‰VPDB (falls between –15.13‰VPDB for 151, 2H, –15.32‰VPDB for A1/H and –15.54‰VPDB for 76H-modeled ones, and –15.35‰VPDB for the measured one, A1/H).

The shift of $\delta^{13}C$ values in reference to atmospheric CO_2 in the climatic conditions of Israel is ca. 7–8‰VPDB. The samples originating from humid environment show lower $\delta^{13}C$: –20.61 (80H) to –23.8 (5H) for modeled values and –21.68 (80H) for the measured one, which may be the result of higher isotopic fractionations during CO_2 diffusion through mortar material. Plasters and external mortars almost do not display high fractionation. The modeled $\delta^{13}C$ for binder in finishing plasters (10H) and for open-air, façade mortars from the outermost layer (61H) are close to –9.3 ± 0.2‰VPDB.

In the environmental conditions similar to inland Israel (with high average annual temperatures and low humidity) it is possible to apply the approximate calculation of the aggregate content relatively to the binder content basing on $\delta^{13}C$ analyses.

Separation of the sufficiently clean binder material from the mortar (both, for ^{14}C and $\delta^{13}C$ measurements) is rather difficult, that is why we propose following protocol for ^{14}C dating of mortars from similar to presented environmental conditions: DoM/p (dating of mortars/based on petrography) and DoM/i (dating of mortars/based on isotopic composition).

DoM/p:

1. Make determination of ^{14}C concentration for mortar bulk material.
2. Prepare thin sections of bulk material adequately representing the sample.
3. Using appropriate software, analyze the total area occupied by carbon containing minerals on the microscopic images of thin sections.
4. Calculate fraction of mass of carbon in binder and aggregate (considering different chemical composition of other carbon containing minerals).

https://doi.org/10.1017/RDC.2019.29 Published online by Cambridge University Press

5. Calculate corrected ^{14}C concentration based on previously estimated in the point 4 fraction and then calculate ^{14}C age of binder.
6. Take into account uncertainties of petrographic correction during calculation of conventional ^{14}C age.

DoM/i:

1. Make sure that environment of your mortar sample is equivalent to the average climatic conditions of Inland Israel.
2. Obtain ^{14}C concentration for bulk mortar material.
3. Extract carbonaceous aggregate material from your samples (or outcrops) and measure $\delta^{13}C$ for this material.
4. Measure $\delta^{13}C$ for bulk material.
5. Estimate type of the mortar (plaster, air-hardening type of mortar, humidity).
6. Assume that the $\delta^{13}C$ for binder in finishing plasters, or outermost fragments of open-air mortars is close to –9.3 ± 0.2‰VPDB, the $\delta^{13}C$ for typical air-hardening mortars and multilayer plasters (not finishing one, with composition similar to mortars) is close to –15.3 ± 0.2‰VPDB.
7. Calculate corrected ^{14}C concentration using Eq. (1.4) and then ^{14}C age for the sample.
8. Take into account uncertainties of petrographic or isotopic correction during calculation of conventional ^{14}C age.

We believe that it is possible to adapt the isotopic method also for ^{14}C dating of hydraulic type of mortars, or for mortars from humid conditions, but it is rather complicated and could be a subject for additional research.

ACKNOWLEDGMENTS

The authors gratefully thank all their colleagues from the Department of Physical and Regional Geology in Poznań. Many thanks go to both teams of radiocarbon laboratories in Gliwice and Poznań for the performed measurements. Special thanks to Prof. Anna Pazdur and Prof. Tomasz Goslar for their support and fruitful discussions. The corresponding author sincerely thanks Jędruś and Marysia Wasilewscy, Janka, Małgosia, and Jurek Michalscy for their support and patience.

SUPPLEMENTARY MATERIAL

To view supplementary material for this article, please visit https://doi.org/10.1017/RDC.2019.29.

REFERENCES

Ambers J. 1987. Stable carbon isotope ratios and their relevance to the determination of accurate radiocarbon dates for lime mortars. Journal of Archaeological Science 14(6):569–576.

Baxter MS, Walton A. 1970. Radiocarbon dating of mortars. Nature 225(5236):937–938.

Ben-Avraham Z, Lazar M, Schattner U, Marco S. 2005. The Dead Sea Fault and its effect on civilization. In: Wenzel F, editor. Perspectives in modern seismology. Lectures Notes in Earth Sciences. Berlin, Heidelberg: Springer-Verlag. Vol. 105, p. 146–167.

Ben-Menahem A. 1991. Four thousand years of seismicity along the Dead Sea Rift. Journal of Geophysical Research Atmospheres 96(B12): 20195–20216.

Bronk Ramsey C. 2009. Bayesian analysis of radiocarbon dates. Radiocarbon 51(1):337–360.

Berger R. 1992. ^{14}C dating mortars in Ireland. Radiocarbon 34(3):880–889.

Cohen-Ofri I, Weiner L., Boaretto E, Mintz G, Weiner S. 2006. Modern and fossil charcoal: aspect of structure and diagenesis. Journal of Archaeological Science 33(3):428–439.

Eppelbaum L, Ben-Avraham Z, Katz Y. 2004. Integrated analysis of magnetic, paleomagnetic and K-Ar data in a tectonic complex region: An example from the Sea of Galilee. Geophysical Research Letters 31:L19602.

Garfunkel Z. 1981. Internal structure of the Dead Sea leaky transform (rift) in relation to plate kinematics. Tectonophysics 80:81–108.

Geological Survey of Israel. 2008. The Geological Map of Israel 1:50000, Teverya, sheet 4-II. Sneh A, editor. Jerusalem.

Guidoboni E, Comastri A. 2005. Catalogue of earthquakes and tsunamis in the Mediterranean area from the 11th to the 15th century. Rome-Bologna, Italy: INGV-SGA. p. 1037.

Guidoboni E, Comastri A, Traina G. 1994. Catalogue of ancient earthquakes in the Mediterranean area up to the 10th Century. Rome-Bologna, Italy: INGV-SGA. p. 504.

Goslar T, Nawrocka D, Czernik J. 2009. Foraminiferous limestones in ^{14}C dating of mortar. Radiocarbon 51(2):857–866.

Hajdas I, Trumm J, Bonani G, Biechele C, Maurer M, and Wacker L. 2012. Roman ruins as an experiment for radiocarbon dating of mortar. Radiocarbon 54:897–903.

Hajdas I, Lindroos A, Heinemeier J, Ringbom Å, Marzaioli F, Terrasi F, Passariello I, Capano M, Artioli G, Addis A, Secco M, Michalska D, Czernik J, Goslar T, Hayen R, Van Strydonck M, Fontaine L, Boudin M, Maspero F, Panzeri L, Galli A, Urbanova P, Guibert P. 2017. Preparation and dating of mortar samples—MOrtar Dating Inter-comparison Study (MODIS). Radiocarbon 59(6):1845–1858.

Heinemeier J, Jungner H, Lindroos A, Ringbom A, Von Konov T, Rud N. 1997. AMS ^{14}C dating of lime mortar. Nuclear Instruments and Methods in Physics Research B 123:487–495.

Heinemeier J, Ringbom Å, Lindroos A, Sveinbjörnsdóttir ÁE. 2010. Successful AMS ^{14}C dating of non-hydraulic lime mortars from the medieval churches of the Åland Islands, Finland. Radiocarbon 52(1):171–204.

Katz O, Amit R, Yagoda-Biran G, Hatzor JH, Porat N, Medvedev B. 2011. Quaternary earthquakes and landslides in the Sea of Galilee area, the Dead Sea Transform: Paleoseismic analysis and implication to the current hazard. Israel Journal of Earth Sciences 58:275–94.

Lindroos A, Heinemeier J, Ringbom Å, Braskén M, Sveinbjörnsdóttir Á. 2007. Mortar dating using AMS ^{14}C and sequential dissolution: examples from medieval, non-hydraulic lime mortars from the Åland Islands, SW Finland. Radiocarbon 49(1):47–67.

Lindroos A, Heinemeier J, Ringbom Å, Brock F, Sonck-Koota P, Pehkonen M, Suksi J. 2011. Problems in radiocarbon dating of Roman Pozzolana mortars. Commentationes Humanarum Litterarum 128:214–230.

Lindroos A, Orsel E, Heinemeier J, Lill J-O, Gunnelius K. 2014. ^{14}C dating of Dutch mortars made from burned shell. Radiocarbon 56(3):959–968.

Marco S, Hartal M, Hazan N, Lev L, Stein M. 2003. Archaeology, history and geology of the A.D. 749 earthquake, Dead Sea transform. Geological Society of America. Geology 31(8):665–668.

Marzaioli F, Lubritto C, Nonni S, Passariello I, Capano M, Terrasi F. 2011. Mortar radiocarbon dating: Preliminary accuracy evaluation of a novel methodology. Analytical Chemistry 83(6):2038–2045.

Marzaioli F, Nonni S, Passariello I, Capano M, Ricci P, Lubritto C, De Cesare N, Eramo G, Castillo JAQ, Terrasi F. 2013. Accelerator mass spectrometry ^{14}C dating of lime mortars: methodological aspects and field study applications at CIRCE (Italy). Nuclear Instruments and Methods in Physics Research B 294: 246–251.

Meiler M. 2011. The deep geological structure of the Golan Heights and the evolution of the adjacent Dead Sea fault systém [PhD thesis]. Tel-Aviv University.

Michalska D, Czernik J. 2015. Carbonates in leaching reactions in context of ^{14}C dating. Nuclear Instruments and Methods in Physics Research B 361:431–439.

Michalska D, Czernik J, Goslar T. 2017. Methodological aspect of mortars dating (Poznań, Poland, MODIS). Radiocarbon 59(6):1891–1906.

Michalska D. 2019. Influence of different pretreatment on mortars dating results. Nuclear Instruments and Methods in Physics Research Section B: Beam Interactions with Materials and Atoms doi: https://doi.org/10.1016/j.nimb.2019.03.038.

Michalska D, Pazdur A, Czernik J, Szczepaniak M, Żurakowska M. 2013. Cretaceous aggregate and reservoir effect in dating of binding materials. Geochronometria 40(1):33–41.

Michalska Nawrocka D, Michczyńska DJ, Pazdur A, Czernik J. 2007. Radiocarbon chronology of the ancient settlement on the Golan Heights. Radiocarbon 49 (2):625–637.

Michelson H, Flexer A, Erez Z. 1987. A comparison of the eastern and western sides of the Sea of Galilee and its implication on the tectonics of

the northern Jordan Rift-Valley. Tectonophysics 141(1–3):125–134.

Młynarczyk J. 2000. Na tropach tajemnic antycznego Hippos. Archeologia żywa 3-4(15):11–14 (In Polish).

Mor D, Michelson H, Druckman Y, Mimran Y, Heimann A, Goldberg M, Sneh A. 1997. Notes on the geology of the Golan heights. Report GSI/15/97. Jerusalem.

Nawrocka D, Michniewicz J, Pawlyta J, Pazdur A. 2005. Application of radiocarbon metod for dating of lime mortars. Journal on Methods and Applications of Absolute Chronology, Geochronometria 24:109–115.

Nawrocka D, Czernik J, Goslar T. 2009. ^{14}C dating of carbonate mortars from Polish and Israeli sites. Radiocarbon 51(2):857–866.

Nonni S, Marzaioli F, Secco M, Passariello I, Capano M, Lubritto C, Mignardi S, Tonghini C, Terrasi F. 2013. ^{14}C mortar dating: the case of the Medieval Shayzar Citadel, Syria. Radiocarbon 55(2):514–525.

Pachiaudi C, Marechal J, Van Strydonck M, Dupas M, Dauchot-Dehon M. 1986. Isotopic fractionation of carbon during CO2 absorption by mortar. Radiocarbon 28(2A):691–697.

Pazdur A, Michczyński A, Pawlyta J, Spahiu P. 2000. Comparision of the radiocarbon dating methods used in the Gliwice Radiocarbon Laboratory. Geochronometria 18:9–14.

Rebollo NR, Cohen-Ofri I, Popovitz-Biro R, Bar-Yosef O, Meignen L, Goldberg P, Weiner S, Boaretto E. 2008. Structural characterization of charcoal exposed to high and low pH: implications for ^{14}C sample preparation and charcoal preservation. Radiocarbon 50(2):289–307.

Reches Z, Hoexter DF. 1981. Holocene seismic and tec tonic activity in the Dead Sea area. Tectonophysics 80:235–254.

Reimer PJ, Bard E, Bayliss A, Beck JW, Blackwell PG, Ramsey CB, Grootes PM, Guilderson TP, Haflidason H, Hajdas J, Hattž C, Heaton TJ, Hoffmann DI, Hogg AG, Hughen KA, Kaiser KF, Kromer B, Manning SW, Niu M, Reimer RW, Richards DA, Scott EM, Southon JR, Staff RA, Turney CSM, Van der Plicht J. 2013. IntCal13 and Marine13 radiocarbon age calibration curves 0–50,000 years cal BP. Radiocarbon 55(4):1869–1887.

Ringbom Å, Heinemeier J, Lindroos A, Brock F. 2011. Mortar dating and Roman pozzolana. Current research on Roman mortar and concrete. Proceeding of the conference March 27–29, 2008 Helsinki. In: Ringbom Å, Hohlfelder RL, editors. Societas Scientiarum Fennica. Commentationes Humanarum Litterarum. Vol. 128, p. 187–206.

Ringbom Å, Lindroos A, Heinemeier J, Sonck-Koota P. 2014. 19 years of mortar dating: learning from experience. Proceedings of the Radiocarbon and Archaeology 7th International Symposium Ghent, Belgium, April 2013. Radiocarbon 56(2):619–635.

Segal A, Młynarczyk J, Burdajewicz M, Schuler M, Eisenberg M. 2004. Hippos (Sussita). Fifth season of excavations and summary of all five seasons (2000–2004). Haifa: University of Haifa, Zinman Institute of Archaeology (In Hebrew and English).

Shaliv G. 1991. Stages in the tectonic and volcanic history of the Neogene Basin in the Lower Galilee and the Valleys. Jerusalem: Geological Survey of Israel. GSI/11/91, p. 94 (In Hebrew with English abstract).

Shtober-Zisu N. 2013. The geographical, geological and geomorphological settings of the Sussita region. In: Segal A, Eisenbe M, Młynarczyk J, Burdajewicz M, Schuler M, editors. Hippos—Sussita of the Decapolis. The first twelve seasons of excavations. The Zinman Institute of Archaeology, University of Haifa, Israel. p. 34–40.

Stuiver M, Polach H. 1977. Discussion: reporting of ^{14}C data. Radiocarbon 19(3):355–363.

Van Strydonck M, Dupas M, Dauchot-Dehon M, Pachiaudi Ch, Marechal J. 1986. The influence of contaminating fossil carbonate and the variations of $\delta^{13}C$ in mortar dating. Radiocarbon 28(2A):702–710.

Van Strydonck M, Dupas M, Keppens E. 1989. Isotopic fractionation of oxygen and carbon in lime mortar under natural environmental conditions. Radiocarbon 31(3):610–618.

Wechsler N, Katz O, Dray Y, Gonen I, Marco S. 2009. Estimating location and size of historical earthquake by combining archaeology and geology in Um-El-Qanatir, Dead Sea Transform. Natural Hazards 50:27–43.

https://doi.org/10.1017/RDC.2019.29 Published online by Cambridge University Press